Identification and Characterization of Designer Phencyclidines (PCPs) in Forensic Casework

Edward Sisco[a*], Aaron Urbas[a]
[a]National Institute of Standards and Technology, Gaithersburg, MD, USA
edward.sisco@nist.gov / DrugID@nist.gov
ORCIDs: Sisco (0000-0003-0252-1910), Urbas (0000-0003-1535-5376)

For submission to: Emerging Trends in Drugs, Addictions, and Health *or* Drug Analysis and Testing

Graphical Abstract

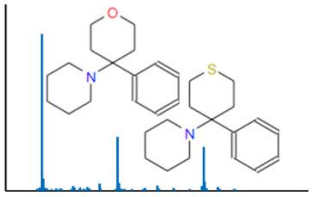

Highlights

- Three new PCP analogs (POXP, PTHP, and P2AP) were identified and characterized
- All compounds were found to have substitutions on the cyclohexyl ring
- Characterization was completed using DART-MS, NMR, GC-MS, and GC-FID

Abstract

With the sustained prevalence and introduction of new emerging drugs throughout the world there is a need for continued development and maintenance of platforms that enable rapid identification and characterization of unknown compounds. To complement existing efforts, a collaborative platform between the National Institute of Standards and Technology (NIST) and practicing forensic agencies is being deployed which enables laboratories to leverage techniques and expertise that may not exist at their facilities. Using this approach, unknown compounds are identified and characterized using a suite of analytical tools to obtain (1) a rapid preliminary identification followed by (2) a more complete characterization and confirmation of the preliminary identification. To demonstrate this platform, the characterization of three previously unreported analogs of phencyclidine (PCP) are described. A preliminary identification of the three substances was obtained using direct analysis in real time mass spectrometry (DART-MS) with confirmation by nuclear magnetic resonance (NMR) spectroscopy, gas chromatography mass spectrometry (GC-MS) and gas chromatography flame ionization detection (GC-FID).

Keywords

Emerging Drugs; Novel Psychoactive Substances; Phencyclidine; PCP; Identification

1. Introduction

Identification of emerging drugs and novel psychoactive substances continue to be a challenge for many forensic laboratories. The drug landscape, as highlighted in several reports [1–4], continues to change at a rapid pace with new compounds being identified on a regular basis. While the number of new drugs steadily increases, so does the breadth of compound classes these emerging drugs cover. A major challenge for many laboratories lies in the characterization of these new compounds when they are encountered in casework. There are a few laboratories capable of in-depth analyses of new substances, but most lack the required instrumentation, personnel and bandwidth. Moreover, even if a new substance can be identified by a laboratory, there is a distinct possibility that a reference material does not exist for comparative analysis.

To help address this need, the National Institute of Standards and Technology (NIST) is developing a collaborative program that will allow forensic laboratories that do not have the bandwidth and resources to identify unknowns to leverage the expertise and instrumentation available at NIST to assist in identifying and characterizing unknown compounds. Under this program, a suite of analytical tools is used to (1) establish a rapid preliminary identification of an unknown, (2) characterize and confirm the preliminary identification, and (3) measure and provide additional data back to the community that is of use with commonly available instrumentation. Extensions of this program seeks to develop a pipeline for providing well-characterized physical materials back to the community when a commercial source is unavailable. While the platform/program is still being developed, a limited number of unknown materials were provided by practicing forensics laboratories for proof-of-concept. In this work, the identification and characterization of three novel phencyclidine (PCP) analogs is presented.

2. Materials and Methods

2.1 DART-MS

Direct analysis in real time mass spectrometry (DART-MS) measurements were made using an IonSense DART-SVP (Saugus, MA, USA) ion source coupled to a JEOL AccuTOF 4G LC-plus mass spectrometer (Peabody, MA, USA). The samples were

analyzed in both positive and negative ionization modes. For both analyses, helium (99.999 % purity) was used as the source gas with a gas stream temperature of 400 °C and a grid voltage of ±150 V. For the positive mode analysis, a scan range of *m/z* 80 to *m/z* 800 was used along with an RF Guide voltage of +700 V, a ring lens voltage of +5 V, and an orifice 2 voltage of +5 V. The orifice 1 voltage was cycled (+30 V, +60 V, and +90 V) at 0.2 s $cycle^{-1}$. For negative mode analysis a scan range of *m/z* 30 to *m/z* 550 was used, at 0.2 s $scan^{-1}$ along with an RF Guide voltage of -250 V, an orifice 1 voltage of -30 V, a ring lens voltage of -5 V, and an orifice 2 voltage of -5 V. Data analysis was completed using both the NIST/NIJ DART-MS Data Analysis Tool [5] and Mass Mountaineer (Diablo Analytical, Antioch, CA). The NIST DART-MS Forensics Database (version Dragonfly) was also employed [6].

Samples were analyzed as acetonitrile solutions with an approximate concentration of 1 mg mL^{-1}. Aqueous solutions with an approximate concentration of 1 mg mL^{-1} were also analyzed in negative ionization mode to assist in identifying the salt form of the samples. Polyethylene glycol 600 was used as an *m/z* calibration compound in both ionization modes. A methanolic solution of cocaine (Cayman Chemical, Ann Arbor, MI) with an approximate concentration of 0.1 mg mL^{-1} was used as a positive control in positive ionization mode while a methanolic solution of AB-FUBINACA (Cayman Chemical) with an approximate concentration of 0.1 mg mL^{-1} was used as a positive control in negative ionization mode. Acetonitrile was run as a negative control in both ionization modes.

2.2 NMR

Nuclear magnetic resonance (NMR) measurements were made using a Bruker Avance II 600 MHz NMR equipped with a broadband-inverse (BBI) probe. Single aliquots (approximately 10 mg to 12 mg) of each sample were dissolved in (600 to700) µL of $CDCl_3$ (D, 99.96 %) and used for all NMR analyses. Multiple 1D and 2D spectra were collected to characterize the sample including 1D ^{1}H and ^{13}C, ^{1}H correlated spectroscopy (COSY), ^{1}H-^{13}C heteronuclear single quantum coherence spectroscopy (HSQC), ^{1}H-^{13}C heteronuclear multiple bond correlation spectroscopy (HMBC), and 1D ^{1}H nuclear Overhauser effect spectroscopy (NOE). Acquisition parameters for the experiments are

given in Supplemental Table 1. The residual solvent peak of $CDCl_3$ was used as the ^1H chemical shift reference and assigned a value of 7.260 ppm. The chemical shift axis scales of the remaining nuclei were established according to the IUPAC unified scale from this [7].

2.3 GC-MS and GC-FID

Gas chromatography mass spectrometry (GC-MS) and gas chromatography flame ionization detection (GC-FID) measurements were made using a Thermo Trace 1310 gas chromatograph coupled with a TSQ8000evo mass spectrometer. Helium (99.999 % purity) was used as the carrier gas along with an Agilent DB-35 column (30 m x 0.25 mm x 0.25 µm) for GC-MS and an Agilent DB-5 column (30 m x 0.25 mm x 0.25 µm) for GC-FID. Additional method parameters are provided in Supplemental Tables 2 and 3. Data analysis was completed using a suite of tools from the NIST Mass Spectrometry Data Center including AMDIS, MS Interpreter, and NIST MS Search [8]. Both the NIST20 and SWGDRUG 3.9 [9] mass spectral libraries were employed.

For GC-MS, samples were analyzed as acetonitrile solutions with an approximate concentration of 0.25 mg mL^{-1}. A ≈0.1 mg mL^{-1} methanolic solution of cocaine was used as a positive control. Acetonitrile was used as a negative control. An alkane ladder (C_7-C_{40}) (Sigma-Aldrich) dissolved in hexane was used for retention index calculations.

For GC-FID, samples were analyzed as acetonitrile solutions with an approximate concentration of 2.5 mg mL^{-1}. A ≈1 mg mL^{-1} methanolic solution of cocaine was used as a positive control. Acetonitrile was used as a negative control. An alkane ladder (C_7-C_{40}) dissolved in hexane was used for retention index calculations.

3. Results and Discussion

Three unique samples were analyzed. All were white powders and were labeled as either “POXP”, “PTHP”, and “P2AP”.

3.1 DART-MS

Initial analysis of the samples was completed using DART-MS. When the spectra were searched against the NIST DART-MS Forensics Database no potential matches were identified. The low fragmentation (+30 V) mass spectrum of the samples, POXP and PTHP, shown in Figure 1 and Supplemental Figure 1, produced a distinct pattern consisting of a prominent peak at a nominal *m/z* 86, a prominent presumed molecular ion, and at least one additional fragment ion in the range of *m/z* 150 to *m/z* 200. This pattern is characteristic of PCP and PCP analogs, representing the signature of the intact molecule along with the fragments formed when the protonated piperidine ring (*m/z* 86) is dissociated from the rest of the molecule. This type of fragmentation, at a low orifice energy, is fairly unique to PCP-related compounds. Accurate mass measurements of the ions at *m/z* 86 (*m/z* 86.099 for both samples) were within the ±5 mDa instrument tolerance of the protonated piperidine ion ($[C_5H_{12}N]^+$, *m/z* 86.097). No other reasonable chemical compositions were identified for this ion using the Composition function in Mass Mountaineer.

For P2AP, also shown in Figure 1 and Supplemental Figure 1, the low fragmentation spectrum did not produce a prominent peak at nominal mass at *m/z* 86 but did produce a strong presumed molecular ion and a strong peak corresponding to the presumed molecular ion with a loss of *m/z* 86.

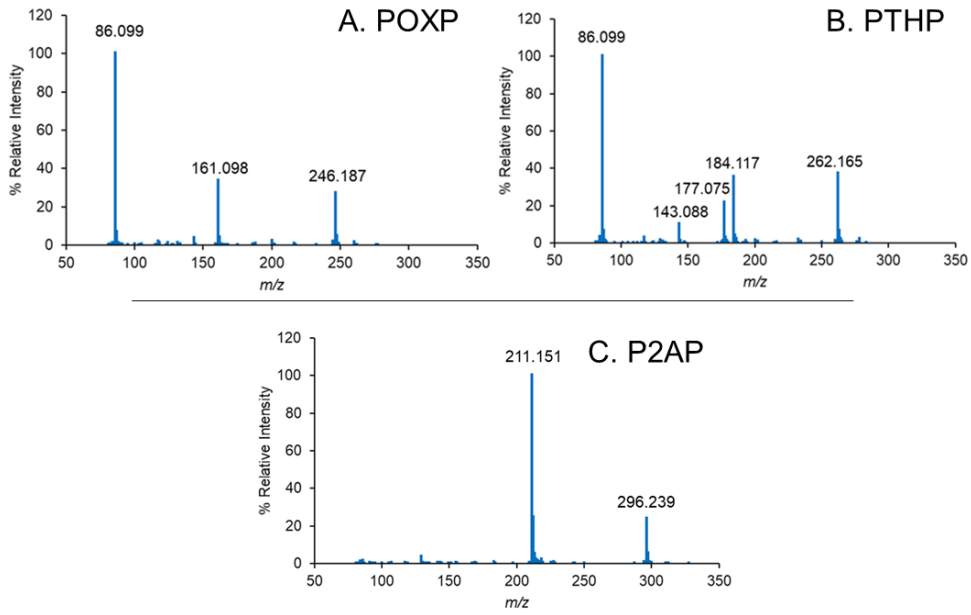

Figure 1. Low fragmentation orifice 1 voltage (+30 V) posititive mode mass spectra of POXP (A., top left), PTHP (B., top right), and P2AP (C., bottom). Comparisons of the observed ions to the theoretical isotopic distributions can be found in Supplemental Figure 1.

The low fragmentation spectrum was then used to identify the presumed molecular formula of the compounds using the assumption that a protonated molecule was formed. For POXP, the assumed protonated molecule was *m/z* 246.187. Potential formulae were identified using a ±5 mDa tolerance, the assumption of an even ion, and constraints of up to 25 carbon atoms, up to four oxygen atoms, at least one but up to four nitrogen atoms (given the piperidine group), up to two sulfur atoms, and up to two fluorine atoms. Three potential formulae were identified ($C_{13}H_{25}NO_2F$, $C_{13}H_{28}NOS$, and $C_{16}H_{24}NO$). Due to the high probability of the presence of a piperidine ring, and given a double bond equivalent of 0.5, $C_{13}H_{28}NOS$ was ruled out. The second major ion (*m/z* 161.098), which was representative of the loss of the piperidine ring, did produce potential formulae consistent with $C_{13}H_{25}NO_2F$ and $C_{16}H_{24}NO$, however, given the structure of PCP and the mass drift similarities between the piperidine ion and the other two ions, $C_{16}H_{24}NO$ was ruled as the probable protonated molecule, and a presumed molecular formula of $C_{16}H_{23}NO$ was obtained.

For PTHP, the presumed protonated molecule was *m/z* 262.165, which yielded potential formulae of $C_{13}H_{22}NO_2F_2$, $C_{13}H_{25}NOSF$, $C_{13}H_{28}NS_2$, $C_{16}H_{21}NOF$, and $C_{16}H_{24}NS$. Both $C_{13}H_{25}NOSF$ and $C_{13}H_{28}NS_2$ were ruled out because they had double bond equivalents of 1.5 and 0.5 respectively. $C_{13}H_{22}NO_2F_2$ and $C_{16}H_{21}NOF$ were ruled out due to poor matches between the measured and theoretical isotope distributions, leading to a presumed protonated molecule with a formula of $C_{16}H_{24}NS$ and a molecular formula of $C_{16}H_{23}NS$.

For P2AP, the presumed protonated molecule was *m/z* 296.239, which yielded potential formulae of $C_{13}H_{31}N_3O_3F$, $C_{15}H_{32}NO_2F$, $C_{18}H_{31}NOF$, $C_{18}H_{34}NS$, and $C_{21}H_{30}N$. The first two formulae were ruled out due to double bond equivalents of -0.5 and $C_{18}H_{34}NS$ was ruled out due to a poor isotopic match. $C_{18}H_{31}NOF$ was ruled out because of a double bond equivalent of 3.5 and the resulting NMR data discussed below. This led to a presumed protonated molecule with a formula of $C_{21}H_{30}N$ and a molecular formula of $C_{21}H_{29}N$.

For all samples, all peaks in the +30 V spectrum above 5 % relative intensity were explainable (Supplemental Figure 1), indicating no major organic contaminants or diluents ionizable by DART were present. The higher orifice 1 voltage mass spectra (+60 V and +90 V) for POXP, PTHP, and P2AP showed general consistency with those of other PCPs and further supported the presumed molecular formulae. The spectra, and corresponding peak tables for the higher orifice 1 voltages, can be found in Supplemental Figures 2 through 4 as well as Supplemental Tables 4 through 6.

Identification of the salt form of the samples was completed by analyzing the aqueous solutions in negative ionization mode. For all three samples, ions at *m/z* 34.967 and *m/z* 36.964, were easily observed, indicating that both samples were hydrochloride salts. The chloride signal was not observed in the water blank.

3.2 NMR

After initial spectral processing, the NMR data from all samples were analyzed for proton counts, proton and carbon peak locations, 1-bond ^{1}H-^{13}C connectivity and ^{1}H-^{1}H and ^{1}H-^{13}C correlations. For all three samples broad proton signals were observed at 11.80 ppm (POXP), 11.66 ppm (PTHP), and 9.25 ppm (P2AP) with no corresponding ^{1}H-^{13}C HSQC correlation that were attributed to a protonated amine in solution. This data and molecular formulae of $C_{16}H_{24}NO$ (for POXP), $C_{16}H_{24}NS$ (for PTHP) and $C_{21}H_{30}N$ (for P2AP) were used in the structure elucidation tool in MNova (14.2.2) to identify potential chemical structures. Note these molecular formulae included an additional proton, based on the protonated amine. For POXP, a single structure was identified with a high match score using the structure elucidation tool and is described in more detail below. For PTHP, two potential structures were identified and compared to the predicted ^{13}C chemical shifts and additional ^{1}H NOE correlations, which both indicated one of the two structures being more likely. For P2AP a single structure was identified with a high match score using the structure elucidation tool. No inconsistencies were found upon further evaluation of the NMR (or MS) data with the probable structures. Additional information about this analysis is provided in the Supplemental Information and elsewhere [10].

The confirmed structure for all three compounds along with atom numbering used for NMR assignments are shown in Figure 2. Note that the atom numbering used in these structures was generated by the MNova structure elucidation tool and based on the associated ^{13}C chemical shift peak positions in descending order. For both POXP and PTHP, the ^{1}H spectrum, shown in Figure 3A and 3B, respectively, exhibited 14 distinct proton signals, some overlapping, attributed to 24 hydrogens including 1 amine, 18 methylene and 5 methine protons. For P2AP, the ^{1}H spectrum, shown in Figure 3C, exhibited 17 distinct proton signals, some overlapping, attributed to 30 hydrogens including 1 amine, 20 methylene and 9 methine protons. Some minor impurity peaks were observed in all samples but the identity of these was not investigated. No counterions were observed in the ^{1}H NMR spectrum for any of the compounds, indicating all three were inorganic salt forms based on the protonated amine. The ^{13}C spectra of POXP and PTHP, shown in Figure 4A and 4B, respectively, exhibited 10 distinct carbon peaks attributed to 16 carbon atoms for both compounds. The ^{13}C spectra of P2AP, shown in Figure 4C, exhibited 14 distinct peaks attributed to 21 carbon atoms.

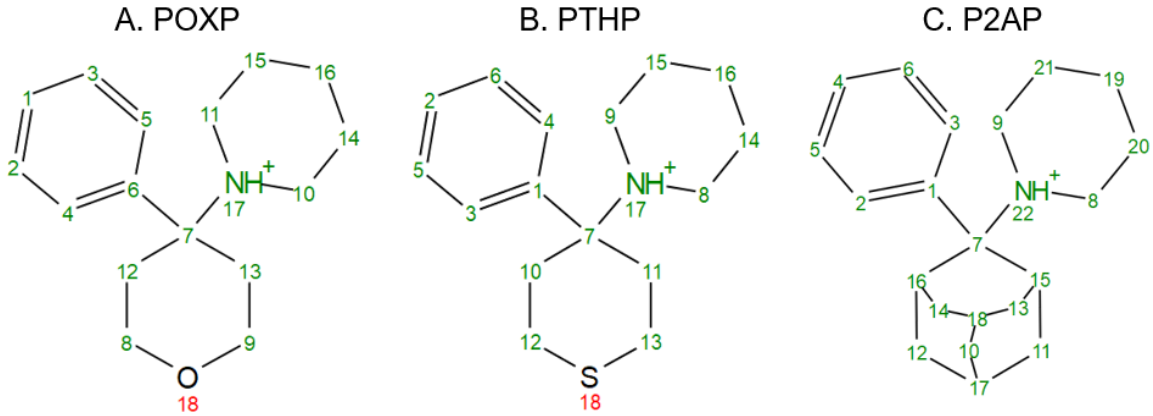

Figure 2. Confirmed structures of POXP (A., left), PTHP (B., center), and P2AP (C., right) with atom numbering used for NMR data peak assignments with observed ^{1}H-^{13}C HMBC indicated by arrows.

For all compounds, proton multiplicity and one-bond ^{1}H-^{13}C correlation was determined through an edited HSQC experiment while connectivity across the structures was established largely through the ^{1}H-^{13}C HMBC spectrum. Additional 1D selective NOE spectra with excitation of the amine proton were also used to confirm connectivity not directly observed in the other 2D data. A scarcity of unambiguous correlations was

recorded for the atoms in the phenyl ring largely due to the narrow chemical shift range of both the protons and carbons, which resulted in difficulty resolving and assigning correlations. The complete collection of 1D and 2D NMR associated with the structure elucidation can be found elsewhere[10].

The 2D NMR data for POXP indicated phenyl, tetrahydropyran and piperidine rings. Supplemental Table 7 provides a summary of the NMR peak assignment data and observed unambiguous 2D correlations. All methylene groups in the molecule exhibited non-symmetric protons. No through-bond correlations were observed between the piperidine ring and the remaining chemical structure. A 1D selective NOE spectrum with excitation of the amine proton (at δ = 11.80 ppm) showed ^{1}H correlations within the piperidine ring (on C10, C11, C14, and C15) as well as on carbons C12 and C13.

For PTHP, the 2D NMR data indicated phenyl, thiane and piperidine rings. Supplemental Table 8 is a summary of the NMR peak assignment data and observed unambiguous 2D correlations. Like POXP, all methylene groups in the molecule exhibited non-symmetric protons. No through-bond correlations were observed between the piperidine ring and the remaining chemical structure. A 1D selective NOE spectrum with excitation of the amine proton (at δ = 11.66 ppm) showed ^{1}H correlations within the piperidine ring (on C8, C9, C14, and C15) as well as on carbons C3, C4, C10, and C11.

For P2AP, the 2D NMR data indicated phenyl and piperidine rings and an adamantyl group. Supplemental Table 9 is a summary of the NMR peak assignment data and observed unambiguous 2D correlations. All but one methylene groups in the molecule exhibited clearly non-symmetric protons. No through-bond correlations were observed between the piperidine ring and the remaining chemical structure. A 1D selective NOE spectrum with excitation of the amine proton (at δ = 9.25 ppm) showed 1H correlations within the piperidine ring (on C8, C9, C20, and C21) as well as on carbons C13, C14, C15, and C16 on the adamantyl group.

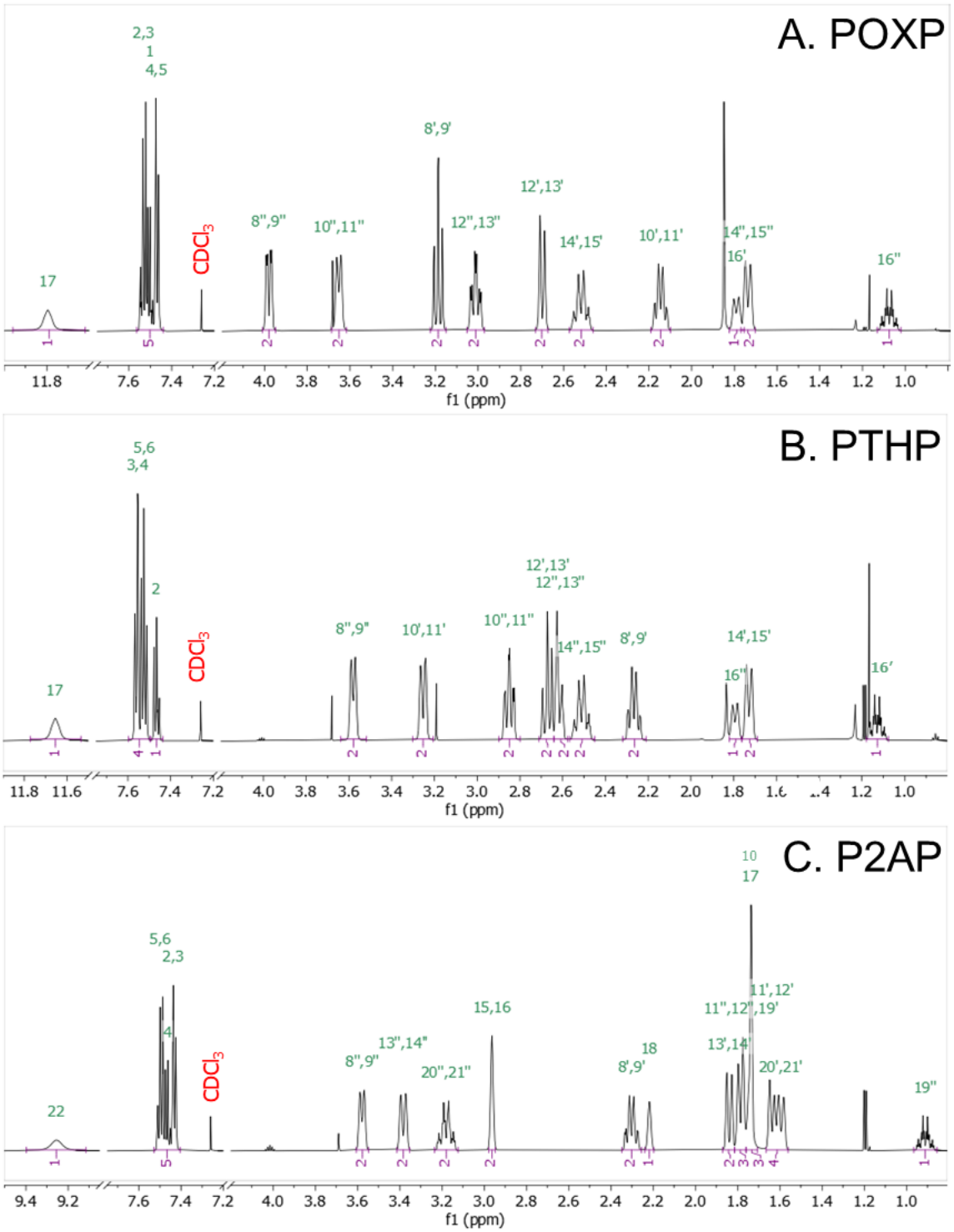

Figure 3. The ^{1}H NMR spectra of POXP (A), PTHP (B), and P2AP (C) in $CDCl_3$. Proton counts of the multiplets are shown beneath the curve and the residual solvent peak is indicatred in red. Assignments based on the atom numbering in Figure 2 are shown above the corresponding multiplets. The displayed spectral range has been trimmed to facilitate comparison.

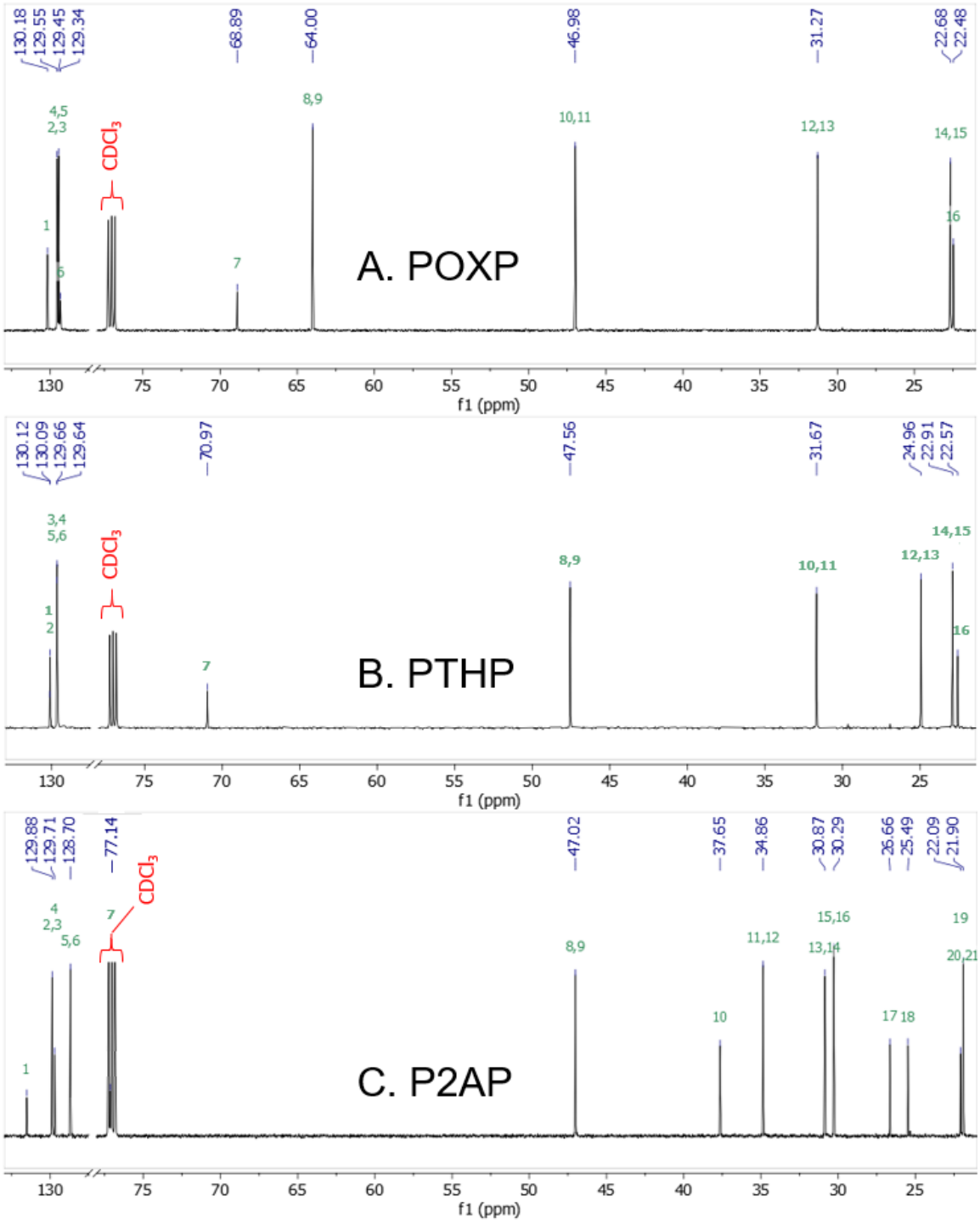

Figure 4. The ^{13}C NMR spectra of POXP (A), PTHP (B), and P2AP (C) in $CDCl_3$. The compound peaks labeled in blue and the solvent peaks red. Assignments based on the atom numbering in Figure 2 are shown above the corresponding peak. The displayed spectral range has been trimmed to facilitate comparison.

3.3 GC-MS

To support the DART-MS and NMR data, as well as obtain additional information about the sample that would be of use to practicing forensic laboratories, GC-MS and GC-FID studies were completed. GC-MS analysis was completed on a more polar DB-35 column. Using the method in Supplemental Table 2, POXP, PTHP, and P2AP were found to have retention times of 11.887 min, 13.483 min, and 14.404 min respectively resulting in retention indices of 2263 a.u, 2546 a.u., and 2723 a.u. For all compounds, as shown in Figure 5, the chromatograms were relatively pure, being dominated by a single major peak.

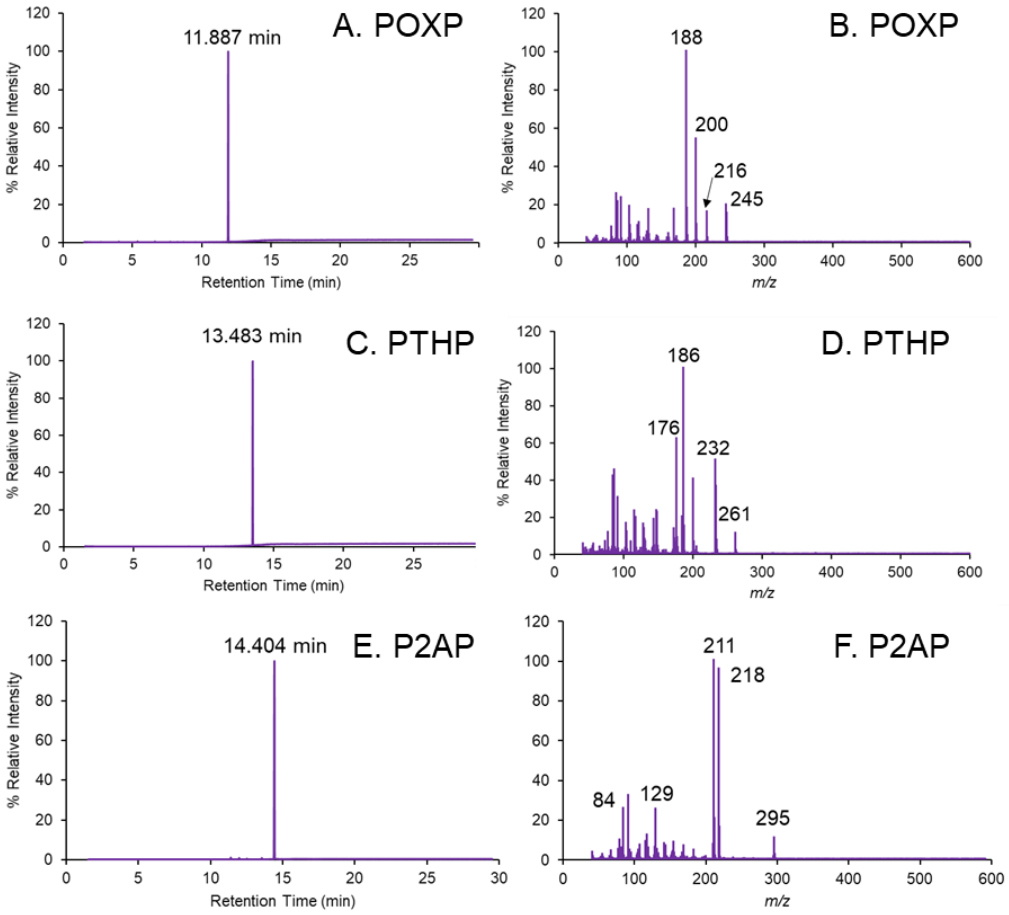

Figure 5. Representative GC-MS chromatograms (A., C., and E., left) and mass spectra (B., D., and F., right) of POXP (A. and B.), PTHP (C. and D.), and P2AP (E. and F.).

The mass spectra generated for all compounds (Figure 5) were first compared to the SWGDRUG version 3.9 and NIST20 spectral libraries using a simple similarity search with NIST MS Search (version 2.3). No reasonable matches were found. Spectra were then searched against the SWGDRUG version 3.9 spectral library using a hybrid similarity

search along with the nominal precursor molecular weights established by DART-MS. Using this search, reasonable matches to phencyclidine (PCP) were obtained with mass shifts of 2 Da for POXP, 18 Da for PTHP, and 52 Da for P2AP, which provided further support of the structure of the compounds and their similarity to PCP. The visual comparisons of the samples to PCP using the hybrid similarity search are provided in Supplemental Figures 5 to 7.

Further evaluation of the GC-MS mass spectra was completed using MS Interpreter [11] along with the structures elucidated from NMR. Evaluation was completed by loading the appropriate mass spectrum and structure into MS Interpreter and assessing the explainability of all peaks above 5 % relative intensity for fragmentation consistency. For POXP the mass spectrum consisted of 18 peaks above 5 % relative intensity, 14 of which could be explained (Supplemental Table 10). The peaks that could not be explained were *m/z* 91, *m/z* 115, *m/z* 116, and *m/z* 129. Using the potential ion list generated for each peak that was not explainable, presumed formulae of $[C_7H_7]^+$, $[C_9H_7]^+$, $[C_9H_8]^+$, and $[C_{10}H_9]^+$ were derived. All four of these ions were also observed in the mass spectrum of PCP in the SWGDRUG version 3.9 mass spectral library.

For PTHP, the mass spectrum consisted of 30 peaks above 5 % relative intensity, all but five of which could be explained. These included *m/z* 91 and *m/z* 116 ions, which were observed in POXP, as well as *m/z* 130 (presumed formula of $[C_{10}H_{10}]^+$, also present in the PCP mass spectrum) and two peaks with unknown formulae at *m/z* 146 and *m/z* 147, both of which had relative intensities of just under 25 % (Supplemental Table 11). For P2AP (Supplemental Table 12), the mass spectrum consisted of 20 peaks above 5 % relative intensity, 14 of which could not be explained using MS Interpreter. The unexplained peaks include many of those observed in POXP and PTHP (as well as PCP) and consisted of hydrocarbon ions.

3.4 GC-FID

A final set of measurements were made on GC-FID using concentrated solutions to further confirm the lack of major impurities and establish retention indices on the commonly used

DB-5 column. Analysis using the method outlined in Supplemental Table 3 produced retention times of 11.286 min, 12.600 min, and 13.603 min for POXP, PTHP, and P2AP respectively, resulting in retention indices of 2171 a.u., 2462 a.u., and 2414 a.u. GC-FID chromatograms, shown in Supplemental Figure 8, indicated no major impurities present in any of the samples.

4. Conclusions

A combination of analytical techniques was employed to characterize three novel PCP analogs. DART-MS proved valuable in establishing the number of compounds present in the sample, the likely molecular formula of the compound(s), the chemical makeup of the major substructures, or fragment ions, and, using comparisons to the NIST DART-MS Forensics Database, identifying the probable class the compound(s) belonged to. The analysis of an aqueous solution also allowed for salt form determination. Knowing that the samples were relatively pure, NMR provided the critical link in establishing the chemical structure of the compound. Subsequent analysis by GC-MS and GC-FID provided further support of the chemical identity of the compounds and established baseline measurements using techniques commonly employed in practicing forensic laboratories. The success of this workflow to rapidly identify and then confirm the presence of these three phencyclidine analogs demonstrated the potential for success of this newly developed program to enable the rapid identification and characterization of emerging drugs.

Additional supporting data, as well as the raw and processed spectra, can be found at the following link: https://doi.org/10.18434/mds2-2527.

5. Acknowledgments

The authors would like to acknowledge Dr. Arun S. Moorthy, Miss Amber Burns, and Dr. David Sparkman for their insight and discussion throughout this study.

6. Disclaimer

Certain commercial products are identified in order to adequately specify the procedure; this does not imply endorsement or recommendation by NIST, nor does it imply that such products are necessarily the best available for the purpose.

7. References

[1] E. Barenholtz, A.J. Krotulski, P. Morris, N.D. Fitzgerald, A. Le, D.M. Papsun, B.K. Logan, W.E. Hahn, B.A. Goldberger, L.B. Cottler, J.J. Palamar, Online surveillance of novel psychoactive substances (NPS): Monitoring Reddit discussions as a predictor of increased NPS-related exposures, International Journal of Drug Policy. 98 (2021) 103393. https://doi.org/10.1016/j.drugpo.2021.103393.

[2] J. Neicun, J.C. Yang, H. Shih, P. Nadella, R. van Kessel, A. Negri, K. Czabanowska, C. Brayne, A. Roman-Urrestarazu, Lifetime prevalence of novel psychoactive substances use among adults in the USA: Sociodemographic, mental health and illicit drug use correlates. Evidence from a population-based survey 2007–2014, PLOS ONE. 15 (2020) e0241056. https://doi.org/10.1371/journal.pone.0241056.

[3] A.J. Krotulski, S.J. Varnum, B.K. Logan, Sample Mining and Data Mining: Combined Real-Time and Retrospective Approaches for the Identification of Emerging Novel Psychoactive Substances, Journal of Forensic Sciences. 65 (2020) 550–562. https://doi.org/10.1111/1556-4029.14184.

[4] P.I. Dargan, D.M. Wood, Novel Psychoactive Substances: Classification, Pharmacology and Toxicology, Academic Press, 2021.

[5] E. Sisco, A.S. Moorthy, S.S. Tennyson, R. Corzo, NIST/NIJ DART-MS Data Interpretation Tool, (2021) 1 files, 373.6 MB. https://doi.org/10.18434/MDS2-2448.

[6] E. Sisco, A.S. Moorthy, NIST DART-MS Forensics Database (is-CID), (2020) 5 files, 124.1 MB. https://doi.org/10.18434/MDS2-2313.

[7] R.K. Harris, E.D. Becker, S.M.C. De Menezes, P. Granger, R.E. Hoffman, K.W. Zilm, International Union of Pure and Applied Chemistry Physical and Biophysical Chemistry Division, Further conventions for NMR shielding and chemical shifts (IUPAC Recommendations 2008), Magn Reson Chem. 46 (2008) 582–598. https://doi.org/10.1002/mrc.2225.

[8] Mass Spectrometry Data Center, NIST, (n.d.). https://chemdata.nist.gov/ (accessed August 26, 2020).

[9] SWGDRUG MS Library, UNited States Department of Justice Drug Enforcement Administration, n.d. https://www.swgdrug.org/ms.htm.

[10] E. Sisco, A.A. Urbas, Project REMEDY - Supplemental Information and Data, (2021) 6 files, 126.1 MB. https://doi.org/10.18434/MDS2-2527.

[11] Mass Spectrum Interpreter Version 2, (n.d.). https://chemdata.nist.gov/mass-spc/interpreter/ (accessed February 28, 2022).

Supplemental Information For:

Identification and Characterization of Designer PCPs in Forensic Casework

Edward Sisco & Aaron Urbas

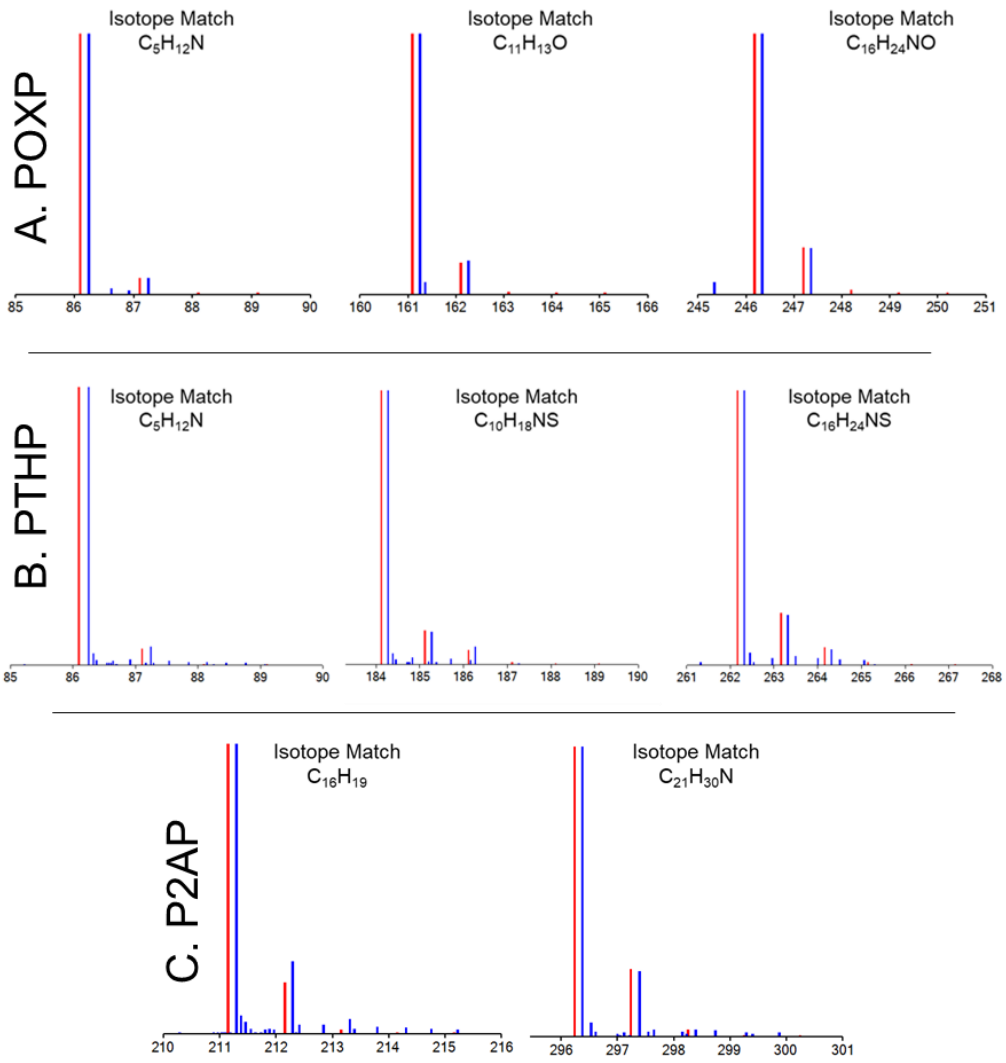

Supplemental Figure 1. Comparison of theoretical (red) to measured (blue) isotopic distributions for major ions in the low fragmentation (+30 V) DART-MS mass spectra of POXP (A., top), PTHP (B., middle), and P2AP (C., bottom). Theoretical isotopic distributions were calculated using Mass Mountaineer.

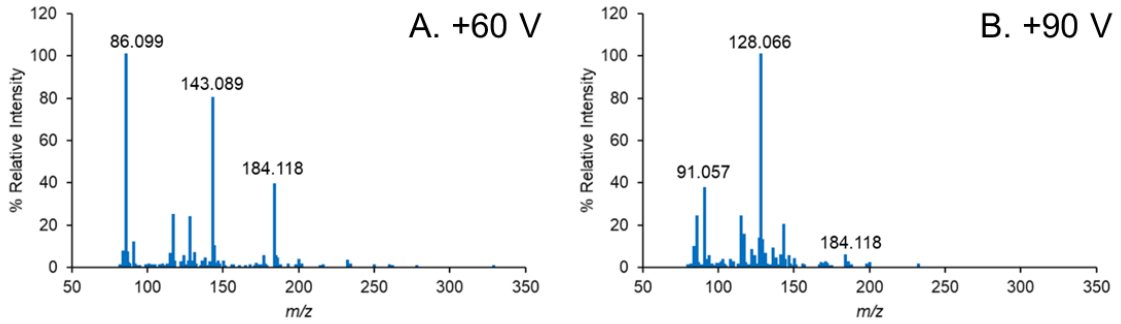

Supplemental Figure 2. Mid-range (+60 V) (A.) and high (+90 V) (B.) fragmentation orifice 1 voltage positive mode spectrum of POXP. Select peaks of interest are identified.

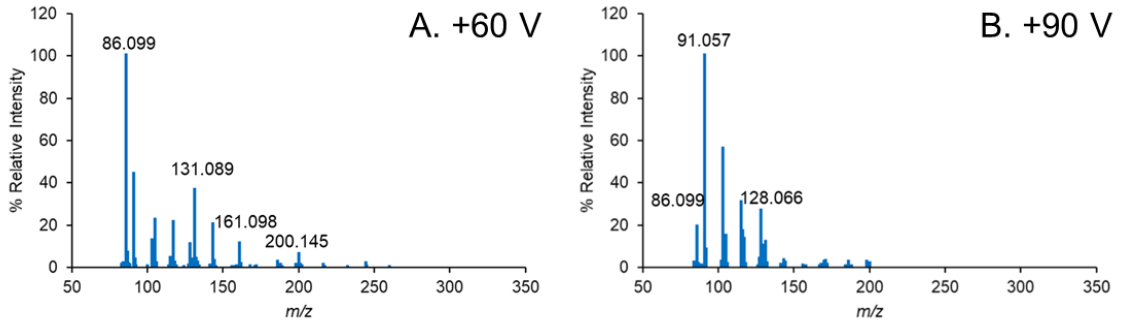

Supplemental Figure 3. Mid-range (+60 V) (A.) and high (+90 V) (B.) fragmentation orifice 1 voltage positive mode spectrum of PTHP. Select peaks of interest are identified.

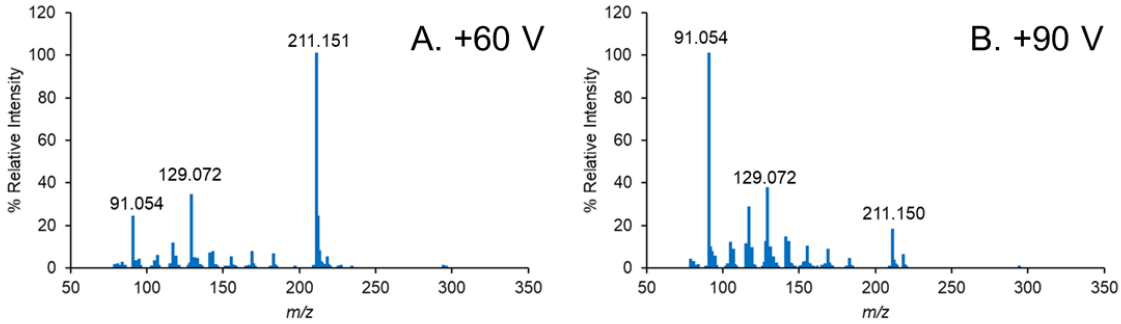

Supplemental Figure 4. Mid-range (+60 V) (A.) and high (+90 V) (B.) fragmentation orifice 1 voltage positive mode spectrum of P2AP. Select peaks of interest are identified.

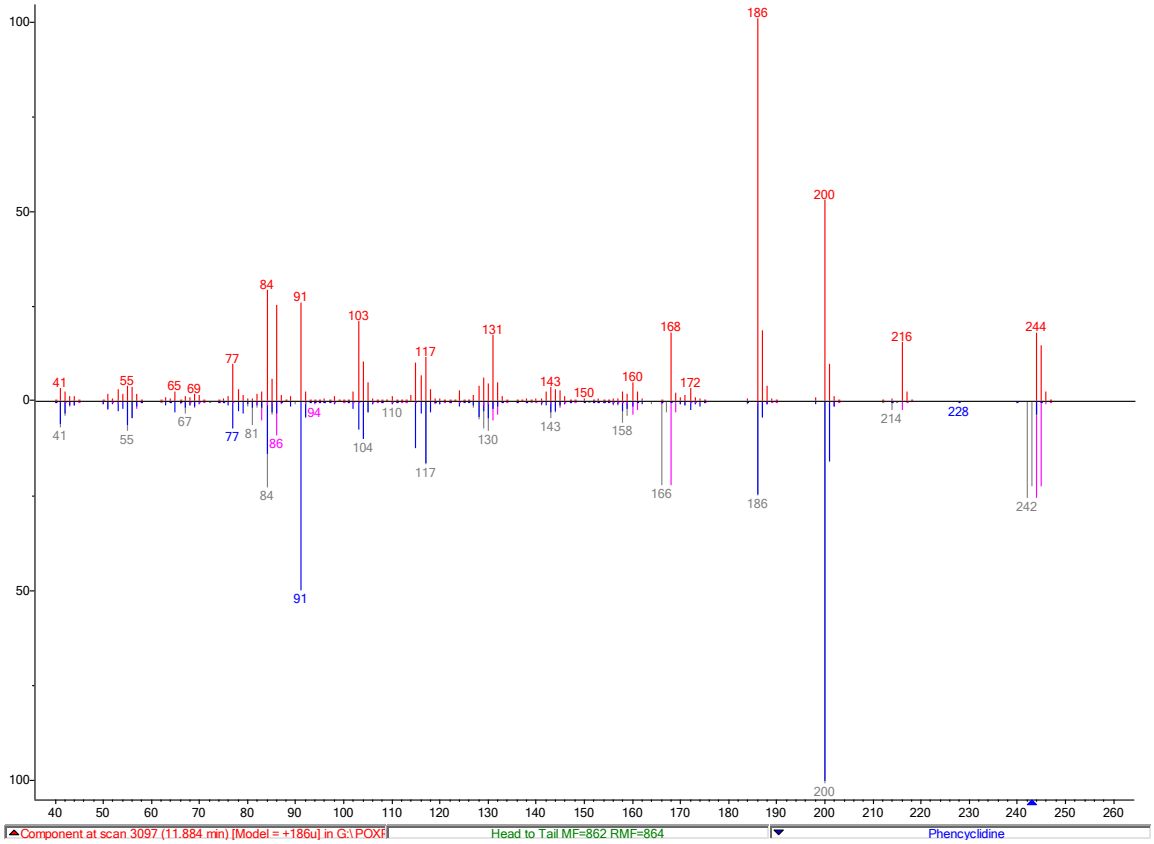

Supplemental Figure 5. Comparison of POXP (top, red) to phencyclidine (bottom, blue) using a hybrid similarity search with a precursor molecular weight of 245 Da. Peaks labeled in pink show those from the phencyclidine mass spectrum in grey that were shifted to align the mass spectra of the two compounds.

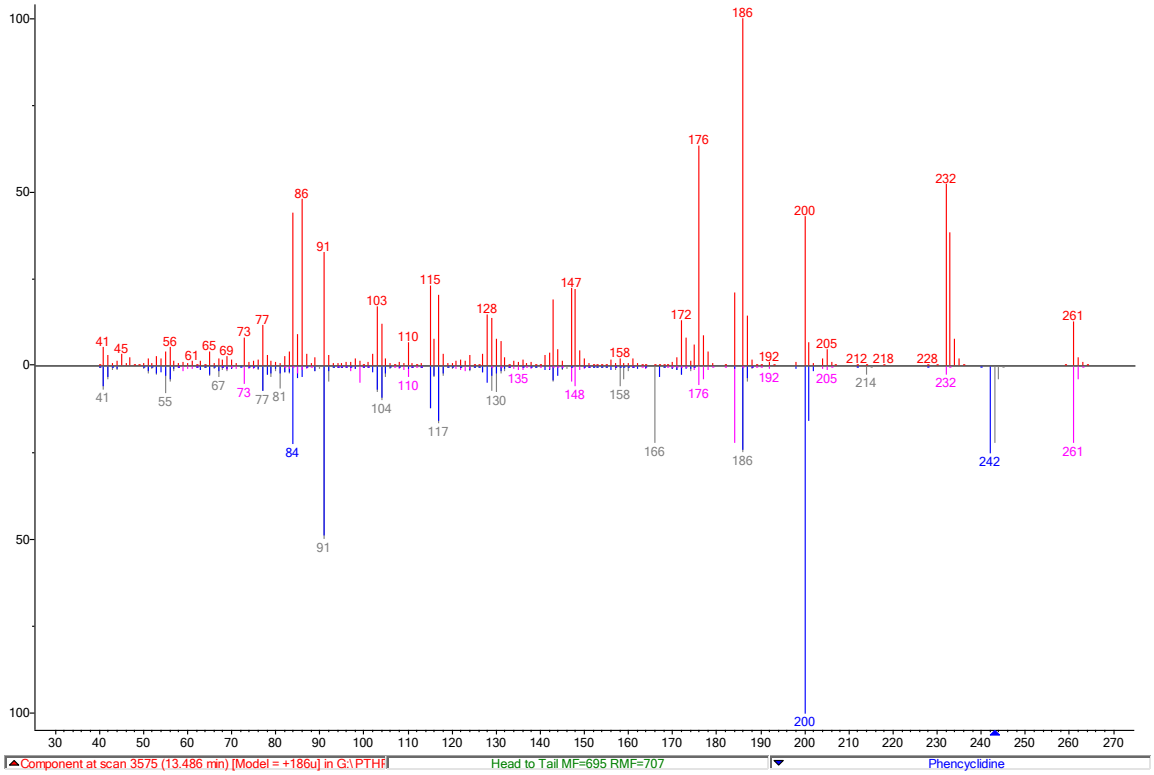

Supplemental Figure 6. Comparison of PTHP (top, red) to phencyclidine (bottom, blue) using a hybrid similarity search with a precursor molecular weight of 261 Da. Peaks labeled in pink show those from the phencyclidine mass spectrum in grey that were shifted to align the mass spectra of the two compounds.

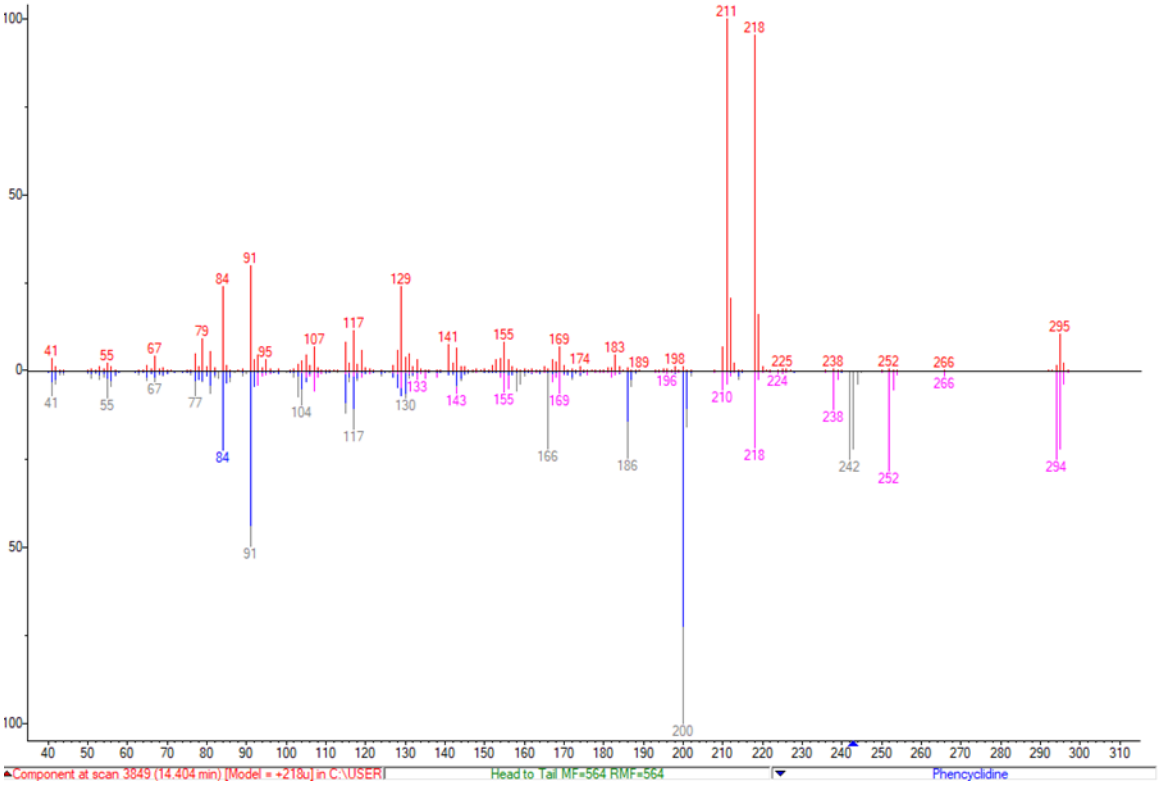

Supplemental Figure 7. Comparison of P2AP (top, red) to phencyclidine (bottom, blue) using a hybrid similarity search with a precursor molecular weight of 295 Da. Peaks labeled in pink show those from the phencyclidine mass spectrum in grey that were shifted to align the mass spectra of the two compounds.

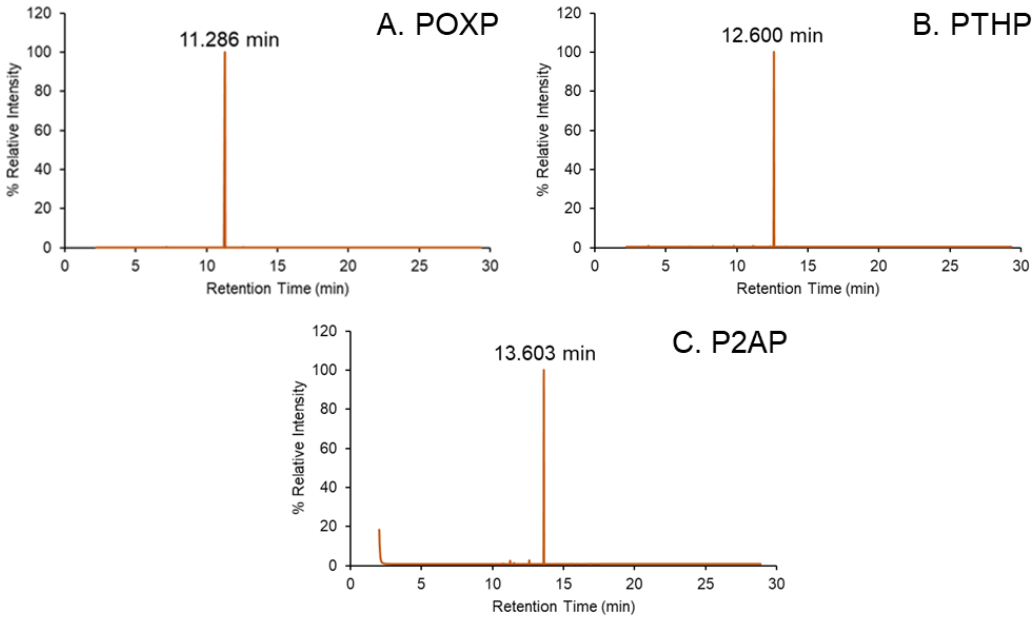

Supplemental Figure 8. GC-FID chromatograms of POXP (A.), PTHP (B.), and P2AP (C.).

Supplemental Table 1. Acquisition parameters for 1D and 2D NMR spectral data for POXP. For PTHP and P2AP, acquisition parameters were largely equivalent apart from the lowest frequency and spectral width, which were automatically optimized during acquisition for the 2D spectra based on the sample specific ^{1}H spectrum.

Parameter	1H 1D	13C 1D	HSQC-EDITED (1H, 13C)	HMBC (1H, 13C)	COSY (1H, 1H)	1H 1D NOE
Pulse Sequence	zg (90 deg pulse)	zgpg (90 deg pulse)	hsqcedetgpsisp2.3	hmbcgplpndqf	cosygpppqf	selnogp
Number of Scans	32	1024	2	8	4	256
Relaxation Delay (s)	25	4	2	1.498	1.9947	2
Acquisition Time (s)	5.4526	0.9088	0.142	0.1331	0.1331	2.7263
Spectrometer Frequency (MHz)	600.13	150.92	(600.13, 150.91)	(600.13, 150.92)	(600.13, 600.13)	600.13
Spectral Width (Hz)	12019.2	36057.7	(7211.5, 24875.6)	(7692.3, 33557.0)	(7692.3, 7692.3)	12019.2
Lowest Frequency (Hz)	-2321.8	-2943.9	(-803.4, -1879.2)	(-15.5, -1717.6)	(28.3, 28.3)	-2321.8
Spectral Width (ppm)	20.03	238.92	(12.02, 164.83)	(12.82, 222.35)	(12.82, 12.82)	20.03
Acquired Size	65536	32768	(1024, 256)	(1024, 256)	(1024, 256)	32768

Supplemental Table 2. GC-MS method parameters.

Temperature Program	1) 80 °C for 0.5 min 2) Ramp 15 °C min^{-1} to 290 °C 3) Hold 15 min
Flow Rate	1.8 mL min^{-1}
Injection Volume	1.0 µL
Inlet Temperature	250 °C
Split Ratio	8:1
Transfer Line	300 °C
Quad Temperature	150 °C
Source Temperature	280 °C
Tune Mode	EI Standard Tune
Solvent Delay	1.5 min
Mass Scan Range	*m/z* 40 – *m/z* 600
Threshold	None
Scan Speed	0.2 s $scan^{-1}$

Supplemental Table 3. GC-FID method parameters.

Temperature Program	1) 80 °C for 0.5 min 2) Ramp 15 °C min^{-1} to 290 °C 3) Hold 15 min
Flow Rate	1.8 mL min^{-1}
Injection Volume	1.0 µL
Inlet Temperature	250 °C
Split Ratio	10:1
Solvent Delay	2.0 min
Data Collection Rate	5 Hz
Detector Temperature	300 ºC
Detector Air Flow Rate	350 mL min^{-1}
Detector N_2 Flow Rate	5 mL min^{-1}
Detector H_2 Flow Rate	10 mL min^{-1}

Supplemental Table 4. Peak list for the mid-range (+60 V) and high (+90 V) fragmentation orifice 1 voltage positive mode spectra of POXP. Formulas and mass drifts (Δ_{mmu}) are also shown. Only peaks above 5 % relative intensity are provided. Presumed formulae were obtained using Mass Mountaineer software. Isotopic peaks above 5 % relative intensity are not listed.

+60 V Spectrum			
m/z	**% Rel. Intensity**	**Presumed Formula**	**Δ_{mmu}**
86.099	100.0	$[C_5H_{12}N]^+$	-1.97
91.057	44.0	$[C_7H_7]^+$	-2.12
103.057	12.7	$[C_8H_7]^+$	-2.69
105.073	22.5	$[C_8H_9]^+$	-2.77
117.073	21.3	$[C_9H_9]^+$	-2.96
128.066	10.9	$[C_{10}H_8]^+$	-3.23
131.089	36.7	$[C_{10}H_{11}]^+$	-3.16
143.089	20.4	$[C_{11}H_{11}]^+$	-2.70
161.098	11.2	$[C_{11}H_{13}O]^+$	-2.27
200.145	6.2	$[C_{14}H_{18}N]^+$	-1.57
+90 V Spectrum			
m/z	**% Rel. Intensity**	**Presumed Formula**	**Δmmu**
86.099	19.2	$[C_5H_{12}N]^+$	-2.09
91.057	100.0	$[C_7H_7]^+$	-2.15
103.057	55.9	$[C_8H_7]^+$	-2.70
105.073	14.9	$[C_8H_9]^+$	-2.75
115.058	30.8	$[C_9H_7]^+$	-2.83
116.065	16.9	$[C_9H_8]^+$	-2.24
117.073	13.3	$[C_9H_9]^+$	-2.58
128.066	26.9	$[C_{10}H_8]^+$	-3.21
129.072	10.2	$[C_{10}H_9]^+$	-2.13
131.086	11.9	$[C_{10}H_{11}]^+$	-3.25

Supplemental Table 5. Peak list for the mid-range (+60 V) and high (+90 V) fragmentation orifice 1 voltage positive mode spectra of PTHP. Formulas and mass drifts (Δ_{mmu}) are also shown. Only peaks above 5 % relative intensity are provided. Presumed formulae were obtained using Mass Mountaineer software. Isotopic peaks above 5 % relative intensity are not listed.

+60 V Spectrum			
m/z	**% Rel. Intensity**	**Presumed Formula**	**Δ_{mmu}**
84.083	7.1	$[C_5H_{10}N]^+$	-2.10
86.099	100.0	$[C_5H_{12}N]^+$	-1.96
91.057	11.4	$[C_7H_7]^+$	-2.09
115.056	5.9	$[C_9H_7]^+$	-2.81
117.073	24.3	$[C_9H_9]^+$	-2.98
128.066	23.4	$[C_{10}H_8]^+$	-3.10
131.089	6.2	$[C_{10}H_{11}]^+$	-3.19
143.089	79.4	$[C_{11}H_{11}]^+$	-2.68
184.118	38.8	$[C_{10}H_{18}NS]^+$	-1.85
+90 V Spectrum			
m/z	**% Rel. Intensity**	**Presumed Formula**	**Δmmu**
84.083	9.1	$[C_5H_{10}N]^+$	-2.03
86.099	23.6	$[C_5H_{12}N]^+$	-2.04
91.057	36.9	$[C_7H_7]^+$	-2.10
115.058	23.6	$[C_9H_7]^+$	-2.80
117.073	15.0	$[C_9H_9]^+$	-3.02
122.100	7.8	$[C_8H_{12}N]^+$	-3.09
127.058	13.2	$[C_{10}H_7]^+$	-3.31
128.066	100.0	$[C_{10}H_8]^+$	-3.13
131.086	5.8	$[C_{10}H_{11}]^+$	-3.26
136.115	8.5	$[C_9H_{14}N]^+$	-2.92
141.073	5.1	$[C_{11}H_9]^+$	-2.83
143.089	19.7	$[C_{11}H_{11}]^+$	-2.76
184.118	5.1	$[C_{10}H_{18}NS]^+$	-1.91

Supplemental Table 6. Peak list for the mid-range (+60 V) and high (+90 V) fragmentation orifice 1 voltage positive mode spectra of P2AP. Formulas and mass drifts (Δ_{mmu}) are also shown. Only peaks above 5 % relative intensity are provided. Presumed formulae were obtained using Mass Mountaineer software. Isotopic peaks above 5 % relative intensity are not listed.

+60 V Spectrum			
m/z	**% Rel. Intensity**	**Presumed Formula**	**Δ_{mmu}**
91.0544	23.6	$[C_7H_7]^+$	0.30
117.0713	10.9	$[C_9H_9]^+$	-0.90
129.0716	33.7	$[C_{10}H_9]^+$	-1.21
141.0714	6.1	$[C_{11}H_9]^+$	-0.96
143.0870	6.8	$[C_{11}H_{11}]^+$	-0.91
169.1024	7.0	$[C_{13}H_{13}]^+$	-0.63
183.1181	5.9	$[C_{14}H_{15}]^+$	-0.71
211.1509	100.0	$[C_{16}H_{19}]^+$	-2.25
+90 V Spectrum			
m/z	**% Rel. Intensity**	**Presumed Formula**	**Δmmu**
91.0547	100.0	$[C_7H_7]^+$	0.07
105.0711	11.4	$[C_8H_9]^+$	-0.70
107.0868	8.1	$[C_8H_{11}]^+$	-0.72
115.0556	10.5	$[C_9H_7]^+$	-0.77
117.0713	28.0	$[C_9H_9]^+$	-0.87
119.0871	8.6	$[C_9H_{11}]^+$	-1.04
128.0634	11.8	$[C_{10}H_8]^+$	-1.17
129.0716	36.8	$[C_{10}H_9]^+$	-1.15
131.0873	9.2	$[C_{10}H_{11}]^+$	-1.20
141.0714	13.8	$[C_{11}H_9]^+$	-0.96
143.0870	11.8	$[C_{11}H_{11}]^+$	-0.93
155.0865	9.4	$[C_{12}H_{11}]^+$	-0.47
169.1025	8.2	$[C_{13}H_{13}]^+$	-0.75
211.1504	17.3	$[C_{16}H_{19}]^+$	-1.81
128.1925	5.5	$[C_{15}H_{24}N]^+$	-1.63

Supplemental Table 7. Summary of NMR peak locations, assignments and observed unambiguous 2D correlations for POXP.

Atom	δ (ppm)	Multiplicity	COSY	HSQC	HMBC
1 C	130.182	1		1	4, 5
H	7.501	1		1	
2 C	129.552	1		2	
H	7.53	1		2	
3 C	129.552	1		3	
H	7.53	1		3	
4 C	129.447	1		4	
H	7.471	1		4	1, 7
5 C	129.447	1		5	
H	7.471	1		5	1, 7
6 C	129.343	1			12', 12", 13'
7 C	68.894	1			4, 5, 8', 8", 9', 9", 12', 12", 13', 13"
8 C	64.001	1		8', 8"	12"
H'	3.187	1	12', 12"	8	7
H''	3.979	1	12', 12"	8	7, 12
9 C	64.001	1		9', 9"	13"
H'	3.187	1	13', 13"	9	7
H''	3.979	1	13', 13"	9	7, 13
10 C	46.978	1		10', 10"	11", 14', 16'
H'	2.145	1	14', 14", 17	10	14
H''	3.652	1	14'	10	11, 16
11 C	46.978	1		11', 11"	10", 15', 16'
H'	2.145	1	15', 15", 17	11	15
H''	3.652	1	15'	11	10, 16
12 C	31.274	1		12', 12"	8"
H'	2.701	1	8', 8"	12	6, 7
H''	3.011	1	8', 8"	12	6, 7, 8
13 C	31.274	1		13', 13"	9"
H'	2.701	1	9', 9"	13	6, 7
H''	3.011	1	9', 9"	13	7, 9
14 C	22.678	1		14', 14"	10'
H'	2.517	1	10', 10", 16"	14	10
H''	1.736	1	10', 16"	14	
15 C	22.678	1		15', 15"	11'
H'	2.517	1	11', 11", 16"	15	11
H''	1.736	1	11', 16"	15	
16 C	22.484	1		16', 16"	10", 11"
H'	1.79	1		16	10, 11
H''	1.075	1	14', 14", 15', 15"	16	
17 N	100	1			
H	11.796	1	8', 9'		
18 O	130.182	1			

Supplemental Table 8. Summary of NMR peak locations, assignments and observed unambiguous 2D correlations for PTHP.

Atom	δ (ppm)	Multiplicity	COSY	HSQC	HMBC
1 C	130.118	1			10", 11"
2 C	130.087	1		2	
H	7.465	1		2	3, 4
3 C	129.662	1		3	2
H	7.554	1		3	7
4 C	129.662	1		4	2
H	7.554	1		4	7
5 C	129.636	1		5	
H	7.523	1		5	
6 C	129.636	1		6	
H	7.523	1		6	
7 C	70.971	1			3, 4, 10', 10", 11', 11", 12', 12", 13', 13"
8 C	47.557	1		8', 8"	16"
H'	2.266	1	8", 14', 14", 17	8	14
H''	3.58	1	8', 14', 14"	8	16
9 C	47.557	1		9', 9"	16"
H'	2.266	1	9", 15', 15", 17	9	15
H''	3.58	1	9', 15', 15"	9	16
10 C	31.674	1		10', 10"	
H'	3.25	1	10", 12"	10	7, 12
H''	2.85	1	10'	10	1, 7, 12
11 C	31.674	1		11', 11"	
H'	3.25	1	11", 13"	11	7, 13
H''	2.85	1	11'	11	1, 7, 13
12 C	24.958	1		12', 12"	10', 10"
H'	2.672	1		12	7
H''	2.612	1	10'	12	7
13 C	24.958	1		13', 13"	11', 11"
H'	2.672	1		13	7
H''	2.612	1	11'	13	7
14 C	22.913	1		14', 14"	8'
H'	1.728	1	8', 8", 14", 16'	14	
H''	2.511	1	8', 8", 14', 16', 16"	14	
15 C	22.913	1		15', 15"	9'
H'	1.728	1	9', 9", 15", 16'	15	
H''	2.511	1	9', 9", 15', 16', 16"	15	
16 C	22.571	1		16', 16"	8", 9"
H'	1.129	1	14', 14", 15', 15", 16"	16	
H''	1.795	1	14", 15", 16'	16	8, 9
17 N	N/A	1			
H	11.655	1	8', 9'		
18 S	N/A	1			

Supplemental Table 9 –Summary of NMR peak locations, assignments and observed unambiguous 2D correlations for P2AP.

Atom	δ (ppm)	Atom Count	COSY	HSQC	HMBC
1 C	131.529	1			5, 6
2 C	129.840	1		2	
H	7.436	1	15, 16	2	7
3 C	129.840	1		3	
H	7.436	1	15, 16	3	7
4 C	129.713	1		4	
H	7.464	1		4	
5 C	128.696	1		5	
H	7.497	1		5	1
6 C	128.696	1		6	
H	7.497	1		6	1
7 C	77.137	1			2, 3, 11", 12", 13', 14', 15, 16
8 C	47.015	1		8', 8"	19", 20", 21"
H'	2.300	1	20", 22	8	20
H"	3.575	1	20', 20"	8	19
9 C	47.015	1		9', 9"	19", 20", 21"
H'	2.300	1	21", 22	9	21
H"	3.575	1	21', 21"	9	19
10 C	37.647	1			13", 14"
H	1.735	2			
11 C	34.858	1		11'	13", 17
H'	1.638	1	13", 15	11	13, 17
H"	1.784	1			7, 17
12 C	34.858	1		12'	14", 17
H'	1.638	1	14", 16	12	14, 17
H"	1.784	1			7, 17
13 C	30.871	1		13', 13"	11'
H'	1.839	1	18	13	7
H"	3.383	1	11', 15	13	10, 11
14 C	30.871	1		14', 14"	12'
H'	1.839	1	18	14	7
H"	3.383	1	12', 16	14	10, 12
15 C	30.285	1		15	
H	2.963	1	2, 3, 11', 13", 18	15	7, 17, 18
16 C	30.285	1		16	
H	2.963	1	2, 3, 12', 14", 18	16	7, 17, 18
17 C	26.661	1		17	11', 11", 12', 12", 15, 16
H	1.737	1	18	17	11, 12, 18
18 C	25.494	1		18	15, 16, 17
H	2.218	1	13', 14', 15, 16, 17	18	
19 C	22.088	1		19"	8", 9"
H'	1.784	1			
H"	0.911	1	20', 20", 21', 21"	19	8, 9, 20, 21
20 C	21.904	1		20', 20"	8', 19"
H'	1.594	1	8", 19"	20	
H"	3.180	1	8', 8", 19"	20	8, 9
21 C	21.904	1		21', 21"	9', 19"
H'	1.594	1	9", 19"	21	
H"	3.180	1	9', 9", 19"	21	8, 9
22 N	N/A	1			
H	9.254	1	8', 9'		

Supplemental Table 10. Peak list for the POXP mass spectrum obtained using GC-MS. Only peaks above 5 % relative intensity are provided. Presumed formulae were obtained using MS Interpreter software and the structure determined by NMR. Peaks above 5 % relative intensity that were attributed to other explainable peaks are not listed. Formulae with an asterisk (*) were not explained using MS Interpreter and were obtained using the potential ion list of MS Interpreter.

m/z	**% Rel. Intensity**	**Presumed Formula**	***m/z***	**% Rel. Intensity**	**Presumed Formula**
77	8.1	$[C_6H_5]^+$	129	5.7	$[C_{10}H_9]^{+*}$
84	25.6	$[C_5H_{10}N]^+$	131	17.2	$[C_{10}H_{11}]^+$
86	21.4	$[C_5H_{12}N]^+$	168	17.5	$[C_{10}H_{18}NO]^+$
91	23.5	$[C_7H_7]^{+*}$	186	100	$[C_{13}H_{16}N]^+$
103	19.0	$[C_8H_7]^+$	200	54.2	$[C_{14}H_{18}N]^+$
104	9.0	$[C_8H_8]^+$	201	9.5	$[C_{13}H_{15}NO]^+$
115	8.9	$[C_9H_7]^{+*}$	216	16.2	$[C_{14}H_{18}NO]^+$
116	5.8	$[C_9H_8]^{+*}$	244	19.7	$[C_{16}H_{22}NO]^+$
117	10.4	$[C_9H_9]^+$	245	15.3	$[C_{16}H_{23}NO]^+$

Supplemental Table 11. Peak list for the PTHP mass spectrum obtained using GC-MS. Only peaks above 5 % relative intensity are provided. Presumed formulae were obtained using MS Interpreter software and the structure determined by NMR. Peaks above 5 % relative intensity that were attributed to other explainable peaks are not listed. Formulae with an asterisk (*) were not explained using MS Interpreter and were obtained using the potential ion list of MS Interpreter.

m/z	% Rel. Intensity	Presumed Formula	*m/z*	% Rel. Intensity	Presumed Formula
41	5.6	$[C_3H_5]^+$	130	8.1	$[C_{10}H_{10}]^{+*}$
56	5.5	$[C_4H_8]^+$	131	6.9	$[C_{10}H_{11}]^+$
73	6.8	$[C_3H_5S]^+$	143	18.8	$[C_7H_{13}NS]^+$
77	11.7	$[C_6H_5]^+$	147	23.5	Unknown
84	42.1	$[C_5H_{10}N]^+$	148	22.5	Unknown
86	45.4	$[C_5H_{12}N]^+$	172	13.8	$[C_{12}H_{14}N]^+$
91	30.5	$[C_7H_7]^{+*}$	173	8.4	$[C_{12}H_{15}N]^+$
103	16.8	$[C_8H_7]^+$	175	6.4	$[C_{12}H_{17}N]^+$
104	12.1	$[C_8H_8]^+$	176	62.1	$[C_{11}H_{12}S]^+$
110	6.7	$[C_7H_{12}N]^+$	184	20.2	$[C_{10}H_{18}NS]^+$
115	23.3	$[C_5H_9NS]^+$	186	100	$[C_{13}H_{16}N]^+$
116	7.7	$[C_9H_8]^{+*}$	200	40.4	$[C_{14}H_{18}N]^+$
117	19.8	$[C_9H_9]^+$	232	50.7	$[C_{14}H_{18}NS]^+$
128	16.3	$[C_6H_{10}NS]^+$	233	36.6	$[C_{14}H_{19}NS]^+$
129	13.8	$[C_6H_{11}NS]^+$	261	11.9	$[C_{16}H_{23}NS]^+$

Supplemental Table 12. Peak list for the mass spectrum obtained using GC-MS. Only peaks above 5 % relative intensity are provided. Presumed formulae were obtained using MS Interpreter software and the structure determined by NMR. Isotopic peaks above 5 % relative intensity are not listed. Formulae with an asterisk (*) were not explained using MS Interpreter.

m/z	**% Rel. Intensity**	**Presumed Formula**
77	5.3	$[C_6H_5]^+$
79	9.9	$[C_6H_7]^{+*}$
81	5.9	$[C_6H_9]^{+*}$
84	25.8	$[C_5H_{10}N]^+$
91	32.3	$[C_7H_7]^{+*}$
107	7.3	$[C_8H_{11}]^{+*}$
115	8.9	$[C_9H_7]^{+*}$
117	12.5	$[C_9H_9]^{+*}$
119	6.0	$[C_9H_{11}]^{+*}$
128	6.2	$[C_{10}H_8]^{+*}$
129	25.3	$[C_{10}H_9]^{+*}$
131	5.2	$[C_{10}H_{11}]^{+*}$
141	7.9	$[C_{11}H_9]^{+*}$
143	6.7	$[C_{11}H_{11}]^{+*}$
155	8.7	$[C_{12}H_{11}]^{+*}$
169	7.0	$[C_{13}H_{13}]^{+*}$
210	7.8	$[C_{16}H_{18}]^+$
211	100	$[C_{16}H_{19}]^+$
218	95.8	$[C_{15}H_{24}N]^+$
295	10.9	$[C_{21}H_{29}N]^+$